GEOPHYSICAL RESEARCH LETTERS, VOL. 26, NO. 24, PAGES 3617-3620, DECEMBER 15, 1999

How Many Waves Are in the Gravity Wave Spectrum?

R. J. Sica and A. T. Russell

Department of Physics and Astronomy, The University of Western Ontario, London, Canada

Abstract. Parametric modelling of density perturbation measurements obtained with the University of Western Ontario's Purple Crow Lidar on 5 nights are used to infer that the typical vertical wavenumber spectrum in the upper stratosphere is dominated by a few quasi-monochromatic waves. In general only 2 of these waves, with growth or decay rates on the order of 1/(14 km) or less, carry most of the spectral energy. These waves are present about half the time on the nights studied. When analyzed using classical spectral techniques these waves appear to form a continuous spectrum. These results may help explain why general circulation models obtain reasonable climatologies when gravity wave parameterization schemes based on a small number of propagating gravity waves are employed.

1. The Problem

Statistical estimation techniques for the vertical wavenumber spectrum of gravity waves, such as the periodogram or, its equivalent, the correlogram, exhibit a m^{-p} power law in the "tail" of the m-spectrum, where p is typically between 2 and 3 (m is the vertical wavenumber and the tail of the spectrum is defined to be the region of the spectrum between approximately 1/(2500 m) and 1/(100 m)). However, this concept of a smooth spectral form in the tail is now being questioned, especially at high temporal and/or spatial resolution. The analysis of high resolution radiosonde measurements by *Vincent et al.* [1997] has suggested that the gravity wave field in the lower stratosphere may actually be composed of a mixture of quasi-monochromatic gravity waves and a broad spectrum. *Sica and Russell* [1999] have also shown that intermittent features with narrow bandwidths often tend to dominate the upper stratospheric m spectrum, although a smooth m^{-3}-type power law exists if sufficient averaging (e.g. hours) is performed.

The presence of only a few "dominant" quasi-monochromatic gravity waves in stratospheric m spectra has also been observed in computer simulations. *Alexander et al.* [1995] have shown that forcing by deep convective processes in squall lines can generate high frequency, narrow bandwidth gravity waves which then propagate into the middle atmosphere with little dispersion. *Prusa et al.* [1996] have shown tropospheric forcing by Gaussian sources such as topographic features or deep convection can also produce quasi-monochromatic waves in the upper stratosphere and mesosphere through dispersive processes.

Characterization of the stratospheric m spectrum has important implications for constraining gravity wave parameterization schemes used in many global circulation models (GCMs), in part because these parametrizations range from those using a small number of monochromatic waves to those with a continuous spectrum of waves. Thus, identifying the vertical wavenumber and bandwidth of the waves comprising the spectrum is an important step towards resolving which parameterization schemes are most realistic.

Prony's method allows individual waves in the spectrum to be estimated from a given data series. In this study the data series are height profiles of density perturbations measured by the Purple Crow Lidar's Rayleigh-scatter system [*Sica et al.* 1995]. A Prony analysis of these density perturbation measurements will then allow us to determine whether or not the spectrum is comprised of a small number or large number of waves.

Paper number 1999GL003683.
0094-8276/99/1999GL003683$05.00

2. Methodology of Gravity Wave Counting

Our primary tool for counting waves in a (potentially) richly featured spectrum is Prony's method [*Marple* 1987]. Prony's method allows one to fit exponentially damped sinusoids to a data series. For each sinusoid a vertical wavenumber, amplitude, growth rate (which is inversely proportional to the wave's bandwidth in the transform domain) and phase are estimated. Details of this procedure and its use in the estimation of gravity wave energy dissipation and eddy diffusion is given by *Sica* [1999].

Does Prony's method estimate damped sinusoids that are physical gravity waves or mathematical basis states that fit the measurements? In the saturated region of the spectrum, the Prony states appear to be gravity waves. As shown by *Sica* [1999] (and as will be evident in the results presented in the next section) these states have wavenumbers, amplitudes and growth rates that are typically associated with gravity waves. However, at smaller scales, Prony's technique attempts to fit states which are a combination of small-scale waves, turbulence, and measurement noise.

The saturated region of the spectrum can be further partitioned using the Hines wavenumber, m_H [*Hines* 1991], where

$$m_H = \frac{N}{V_{\mathrm{rms}}}. \quad (1)$$

Here N is the buoyancy frequency and V_{rms} is the root-mean-square horizontal wind velocity. *Hines* [1991] has shown that when m is greater than the Hines wavenumber, nonlinear processes rapidly dissipate the waves, while, for m less than half the Hines wavenumber, dissipation of the waves by nonlinear processes is very small. We shall, for simplicity's sake, refer to the latter region as the propagating region and the former as the dissipating region. In the propagating region, the amplitude of the wave changes slowly with height (on the order of twice the scale height). In the dissipating region, nonlinear processes and/or critical levels rapidly obliterate the waves. The states found by Prony's method in the propagating region satisfy our expectations for gravity waves, while the states in the dissipating region are a combination of waves, turbulence and measurement noise.

Table 1. Prony Analysis of Upper Stratospheric Vertical Wavenumber Spectra.

Day	Median # of Waves	Minimum # of Waves	Maximum # of Waves	Mean Hines Wavenumber (m^{-1})	Mean Noise Floor ($J/m^3 \cdot m$)	Propagating to Dissipating Power	Dissipating Power to Noise Floor
940830	4	3	5	1.02×10^{-3}	1.43	36	1.2
941012	4	3	5	9.59×10^{-4}	1.64	33	1.2
980207	2	2	3	5.71×10^{-4}	1.33	111	2.5
980428	5	2	6	1.15×10^{-3}	1.04	22	1.4
980802	5	3	6	1.13×10^{-3}	1.22	24	1.4

The characteristics of waves in the propagating and dissipating region will be determined in the following manner. First, individual vertical density perturbation series at 144 m vertical resolution and 1 min temporal resolution (smoothed temporally with a 21-point Kaiser Bessel filter) are fitted by Prony's method to a large number of waves (approximately 30 waves). This high order fit does an extremely good job at fitting the data series with states corresponding to waves, geophysical noise and photon noise (i.e. the RMS fit residuals are much less than the photon noise floor of the measurements). The Hines wavenumber is then calculated for each data series and the sinusoids sorted into propagating and dissipating states. States which have growth rates less than twice the sampling rate, e.g. 1/(288 m), are not included. In practice this choice eliminates only a few heavily damped sinusoids among the thousands of states determined. The density fluctuation fields due to the propagating and dissipating states are then reconstructed and subjected to classical and parametric spectral analyses.

3. Results

Five nights of continuous measurements with 6 to 8 hr time spans in the upper stratosphere (30 to 50 km) were chosen for

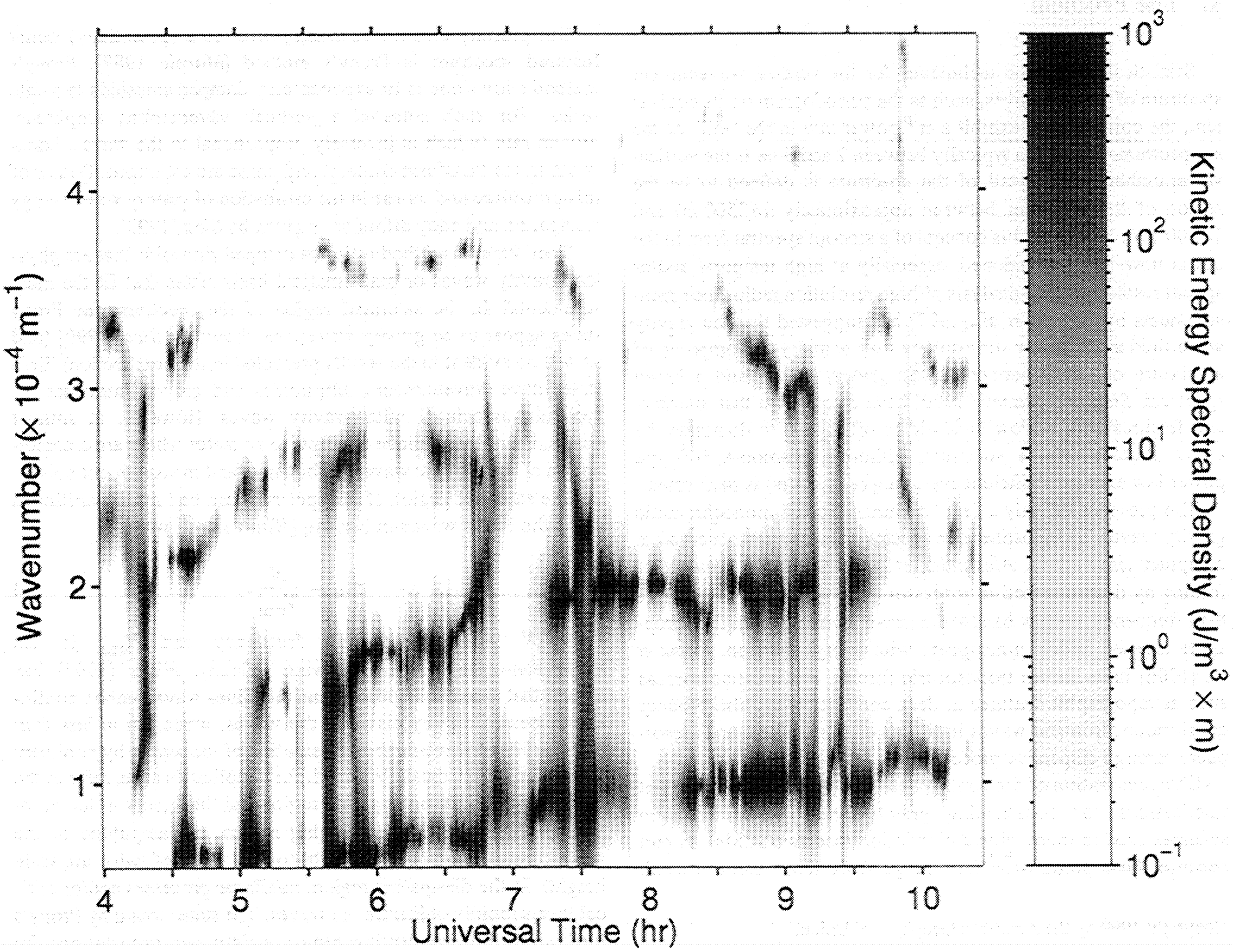

Figure 1. Vertical wavenumber kinetic energy density spectra inferred from the Prony fit to the measurements in the propagating regime on October 12, 1994. The spectra were determined using a modified covariance autoregressive model. A color version of this figure is available at http://pcl.physics.uwo.ca.

Table 2. Vertical Wavelengths (km) of the Two Most Significant Propagating Waves.

	Long Wave			Short Wave		
Day	Lower Wavelength	Mean Wavelength	Upper Wavelength	Lower Wavelength	Mean Wavelength	Upper Wavelength
940830	8	10	16	4	5	8
941012	9	13	17	5	6	7
980207	6	9	12	4	4.5	5
980428	8	11	14	3.5	5	7
980802	9	12	16	4	5	6

analysis (Table 1). Typically the propagating part of the spectrum contains 4 or 5 waves, though on February 7, 1998, only 2 waves were normally present. The lack of waves on February 7, 1998 is due to the smaller Hines wavenumber, which reflects the larger power on this night when compared to the other more "typical" nights.

Figure 1 shows the time evolution of the m spectrum that has been estimated from the reconstructed propagating wave density fluctuation field on the night of October 12, 1994. The median number of propagating waves on this night was 4, with most of the power being carried by the 2 lowest wavenumber waves, one at nominally 1/(10,000 m), the other at 1/(5,000 m). The other 2 waves represent the intermittent features occurring at wavenumbers below 1/(5,000 m). These features have peaks about 2 to 3 times lower than the low wavenumber peaks. The absolute value of the low wavenumber wave's growth rate is on the order of 1/(14 km) (or less), which corresponds to a relatively undamped sinusoid. The other nights studied are similar to October 12, 1994 in that they contain 2 dominant longer wavelength waves, with small growth rates. The intermittency of these waves is also similar to that shown in Figure 1. An attempt to succinctly summarize the other nights is given in Table 2, where the nominal "mean" wavelength is given, as well as a range of wavelengths over which the feature is present.

The ratio of power in the propagating to the dissipating region of the spectrum is given in Table 1. Typically about 30 times more power is found in the propagating region of the spectrum when

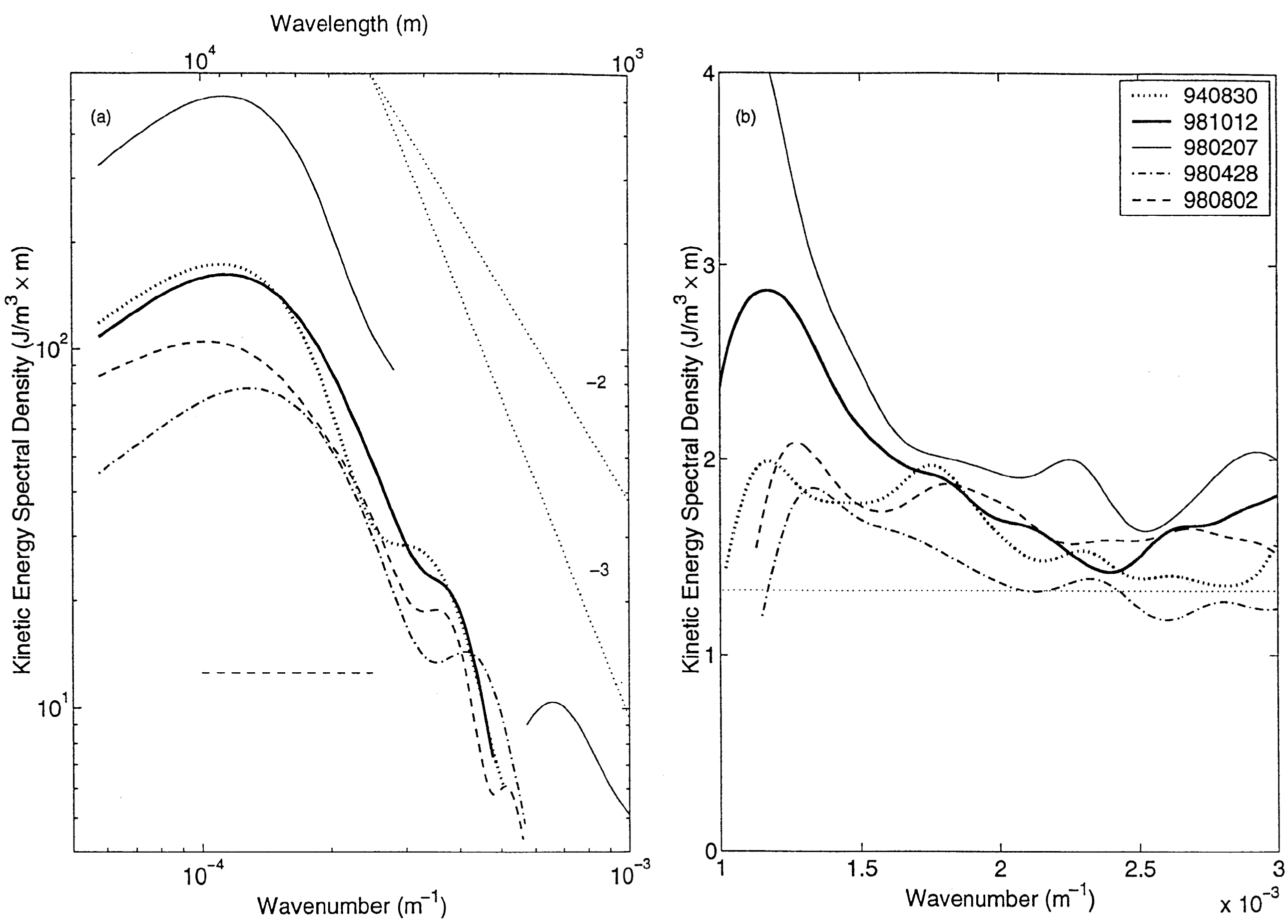

Figure 2. Mean correlograms for the propagating (Panel a) and dissipating (Panel b) spectral regions for the 5 nights listed in Table 1. On Panel (a) the dotted lines indicate power laws with exponents of -2 and -3, while the dashed line indicates the spectral resolution. On Panel (b) the mean photon noise floor for the 5 nights is indicated by the horizontal dotted line. The mean noise floor for each night is given in Table 1. Part of the dissipating spectrum for February 7, 1998 is also shown on Panel (a).

compared to the dissipating region. Figure 2 shows the average correlograms of the propagating and dissipating region of the spectrum for the 5 nights. The propagating correlograms have been computed at a high lag and truncated at half the Hines wavenumber. The dissipating spectra have been computed at a lower lag. The propagating correlograms (Figure 2*a*) show that the combination of only a few waves with low to moderate bandwidths appear to form a continuous, saturated spectrum with power law exponents in the range of -3 to -2, highlighting the low spectral resolution of this technique (here 1.5×10^{-4} m^{-1}). For example, the two lowest wavenumber waves on October 12, 1994 were present over most of the night, but the average correlogram (Figure 2*a*) cannot resolve the two waves at 1/(10,000 m) and 1/(5,000 m). This blending of only a few waves into a m^{-3} power law is due to the low resolution of the correlogram and occurred on all of the nights considered.

Figure 2*b* also shows that although the dissipating region of the spectrum has significantly less power than the propagating region, the power in the dissipating region is still greater than the photon noise floor of the measurements by 20 to 50% (Table 1). The correlograms associated with the dissipating region of the spectrum are essentially white. Occasionally intermittent features appear around the Hines wavenumber, but these features have peak powers of only a few times the noise floor.

4. Conclusions and Discussion

The five nights considered for this study show that, in the upper stratosphere, most of the gravity wave spectral energy is carried by 2 waves with small growth rates. Waves with wavenumbers greater than 1/(1000 m) carry relatively little power and generate a white-noise spectrum. The spectrum is intermittent. The 2 dominant waves are usually present over half of the measurement period.

When the spectrum of the propagating waves is calculated using a low resolution spectral technique, such as the correlogram or periodogram, the average spectrum can be represented as a power law with an exponent of between -3 and -2. However, this power law is associated with the low spectral resolution of the analysis technique and may not be representative of a continuous spectrum of waves. High resolution parametric modelling techniques are better able to isolate the individual waves in the spectrum.

This dominance of a few quasi-monochromatic waves in upper stratospheric *m* spectra may help explain why Lindzen-type parametrizations [e.g. *Lindzen* 1981] appear to work in global circulation models. For example, *Hamilton* [1997] has shown that the climatology of the GDFL SKYHI general circulation model at high spatial resolution with no explicit gravity wave parameterization scheme (i.e. the model generates its own gravity waves which can then interact with the mean wind) is in agreement with a lower resolution SKYHI calculation using a simple Lindzen-type parameterization scheme with 10 waves. Our measurements suggest that a realistic gravity wave parameterization scheme needs to account for the discrete and continuous nature of the spectrum, as well as its associated intermittency.

Acknowledgments. We would like to thank Dr. S. Eckermann for his insightful comments on this work. We would also like to thank the National Science and Engineering Research Council, the Atmospheric Environment Service and the Centre for Research in Environmental Science and Technology (CRESTech) for their financial support and Mr. D. Kwarciak for his graphics wizardry.

References

Alexander, M. J., J. R. Holton and D. R. Durran, The gravity wave response above deep convection in a squall line simulation, *J. Atmos. Sci.*, *52*, 2212-2226, 1995.

Hamilton, K., The role of parameterized drag in a troposphere-stratosphere-mesosphere general circulation model, in *Gravity Wave Processes. Their Parameterization in Global Climate Models*, edited by K. Hamilton, Springer-Verlag, Berlin, pp. 337-350, 1997.

Hines, C. O., The saturation of gravity waves in the middle atmosphere. Part II: Development of Doppler-spread theory. *J. Atmos. Sci., 48,* 1360-1379, 1991.

Lindzen, R. S., Turbulence and stress due to gravity wave and tidal breakdown, *J. Geophys. Res., 86,* 9709-9714, 1981.

Marple, S. L., *Digital spectral analysis.* Prentice-Hall, Inc., Englewood Cliffs, NJ, Chapter 11, 1987.

Prusa, J. M., P. K. Smolarkiewicz and R. R. Garcia, Propagation and breaking at high altitudes of gravity waves excited by tropospheric forcing, *J. Atmos. Sci., 53,* 2186-2216, 1996.

Sica, R. J., S. Sargoytchev, P. S. Argall, E. F. Borra, L. Girard, C. T. Sparrow, and S.Flatt, Lidar measurements taken with a large-aperture liquid mirror. 1. Rayleigh-scatter system, *Appl. Opt., 34,* 6925-6936, 1995.

Sica, R. J. and A. T. Russell, Measurements of the effects of gravity waves in the middle atmosphere using parametric models of density fluctuations. Part I: vertical wavenumber and temporal spectra, *J. Atmos. Sci., 56,* 1308–1329, 1999.

Sica, R. J., Measurements of the effects of gravity waves in the middle atmosphere using parametric models of density fluctuations. Part II: Energy Dissipation and Eddy Diffusion, *J. Atmos. Sci., 56,* 1330–1343, 1999.

Vincent, R A., S. J. Allen, and S. D. Eckermann, Gravity-wave Parameters in the Lower Stratosphere, in *Gravity Wave Processes. Their Parameterization in Global Climate Models,* edited by K. Hamilton, Springer-Verlag, Berlin, pp. 7-25, 1997.

R. J. Sica and A. T. Russell, Department of Physics and Astronomy, The University of Western Ontario, London, ON, Canada N6A 3K7. (e-mail: sica@physics.uwo.ca)

(Received September 29, 1999; accepted October 19, 1999)

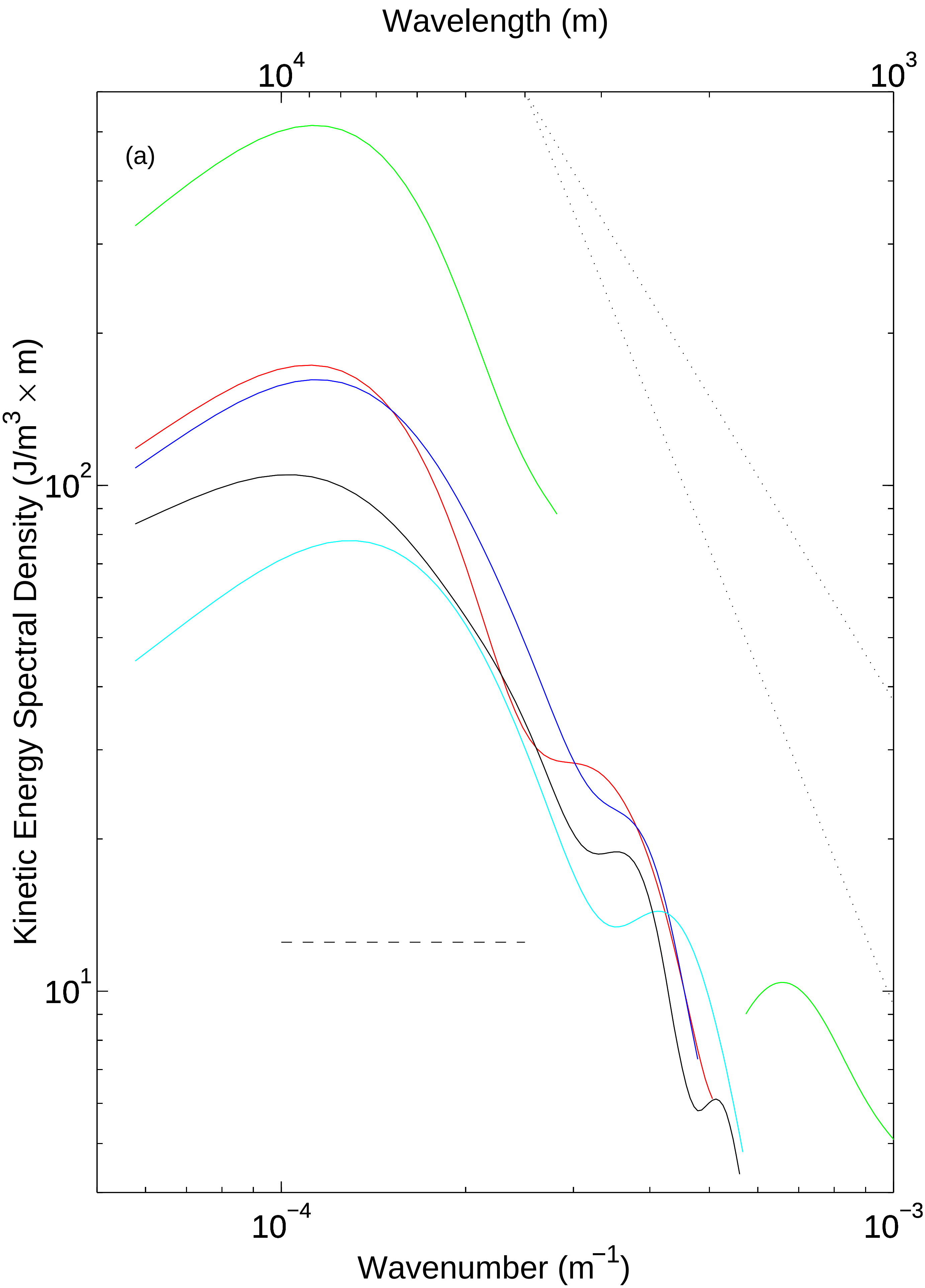

Wavelength (m)
10^4
10^3
(a)
Kinetic Energy Spectral Density (J/m^3 × m)
10^2
10^1
10^-4
10^-3
Wavenumber (m^-1)

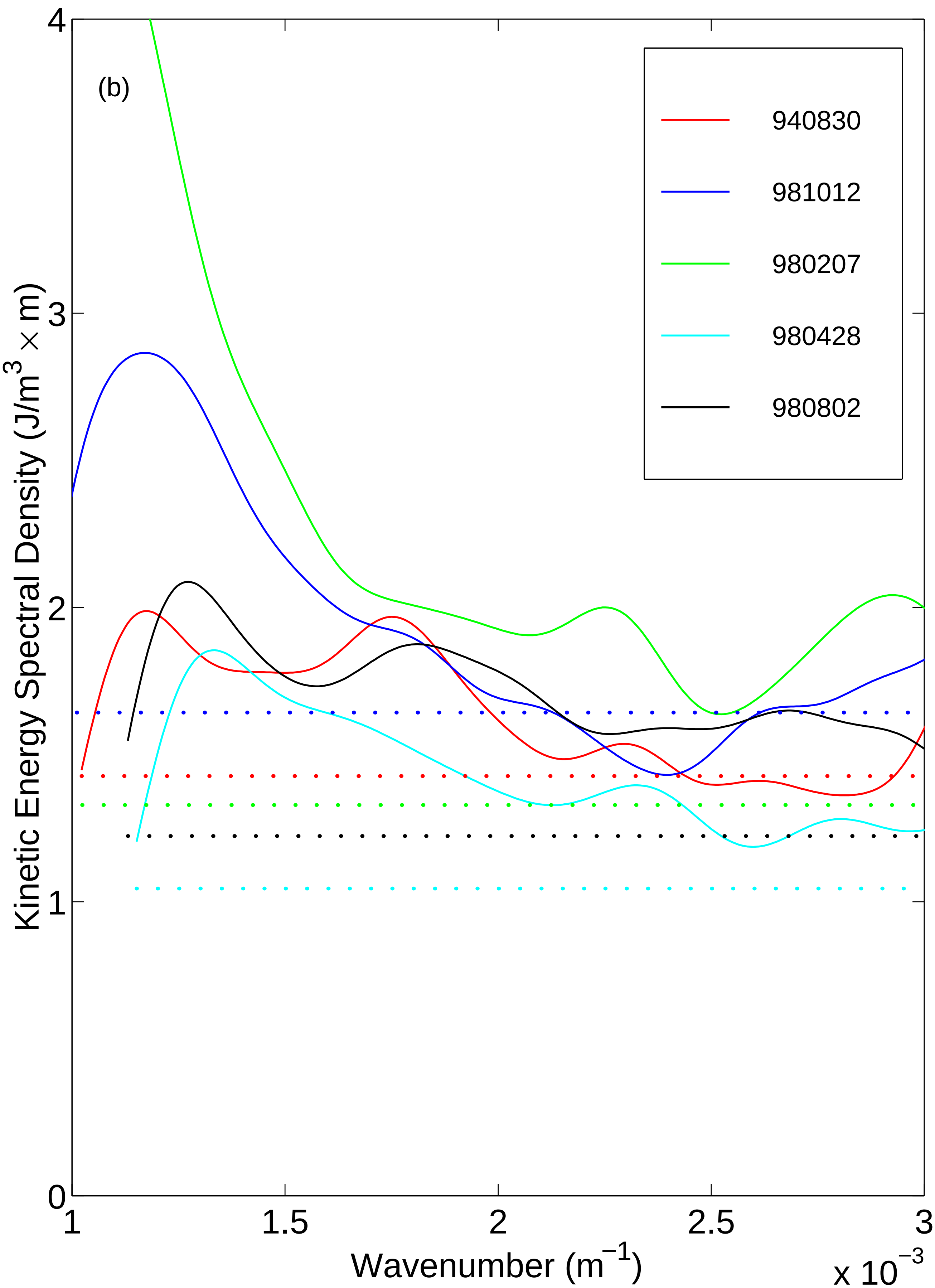

(b)
940830
981012
980207
980428
980802
Kinetic Energy Spectral Density (J/m^3 × m)
Wavenumber (m^{-1})
x 10^{-3}
0
1
2
3
4
1
1.5
2
2.5
3